World Academy of Science, Engineering and Technology
International Journal of Computer and Information Engineering
Vol:9, No:1, 2015

Modeling and Simulation of Standalone Photovoltaic Charging Stations for Electric Vehicles

R. Mkahl, A. Nait-Sidi-Moh, M. Wack

***Abstract*—**Batteries of electric vehicles (BEV) are becoming more attractive with the advancement of new battery technologies and promotion of electric vehicles. BEV batteries are recharged on board vehicles using either the grid (G2V for Grid to Vehicle) or renewable energies in a stand-alone application (H2V for Home to Vehicle). This paper deals with the modeling, sizing and control of a photovoltaic stand-alone application that can charge the BEV at home. The modeling approach and developed mathematical models describing the system components are detailed. Simulation and experimental results are presented and commented.

***Keywords*—**Electric vehicles, photovoltaic energy, lead-acid batteries, charging process, modeling, simulation, experimental tests.

I. Introduction

ELECTRIC vehicles (EVs) are green transports, and they are good means to solve transport and environmental problems. The environmental benefits of EVs increase with the produced electricity from green sources such as (wind, solar, small scale hydroelectricity). Green sources are also a good solution and alternative enabling to avoid the problem of reliability and safely which can be encountered when grid power is used to charge EVs [1]. Charging stations provide power supply for EVs; so, the deployment of complete infrastructures with sophistic equipments is indispensable for promoting EVs. However, EV charging process takes much time than charging process using fuel car [2], and batteries should be efficiently used since the propulsion of EVs depend on their energy storage capacity [3], [23].

EVs can be charged by either plugging into electrical outlets or by means of on-board electricity generation. There are two main places where the batteries of EVs can be charged: either on a car park, corporate or public, or at home. With this last charging solution, a system H2V is designed to charge BEVs using green sources such as photovoltaic systems as illustrated in Fig. 1. In a H2V system, EV can be charged with direct current from photovoltaic panels (PV) or with current from a Lead-Acid battery installed at home (see Fig. 1). Conversely, the system can provide the electric energy from the EV to the household when this is needed (V2H). The study of these charging/discharging processes H2V and V2H systems requires adequate models in order to ensure an optimal energy management and effective usage of the system components. This modeling is based on mathematical equations that govern the system in order to predict and evaluate its behavior.

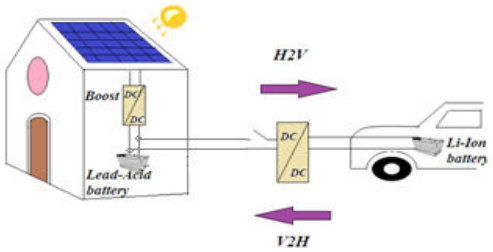

Fig. 1 EV charging/discharging: H2V2H structure

This paper focuses on the modeling and sizing of EV charging stations using solar energy. More precisely, we address a PV panel mathematical model whose parameters are extracted from PV tests. We address also the voltage modeling of lead-acid battery we use in our system H2V. In fact, the battery state information allows optimal control for battery charging/discharging process, reduces the risk of overcharge and deep charging. In addition, it is possible to extend the battery life and reach its optimal usage. To do so, we focus on the modeling of the lead-acid battery voltage by developing a mathematical model enabling to reach these objectives.

The proposed model describes the profile of battery voltage considering time and electrical parameters. These parameters can be found using manufacturer data or experimental tests. Afterward, a mathematical model is deduced using a curve-fitting approach. Many parameters such as the state of charge (SOC), time of charging and discharging, current of charging and discharging should be taken into account during charging and discharging processes.

The remainder of the paper is structured as follows. Section II introduces the energy storage sources. Section III presents the adopted modeling approach. PV and Lead-Acid battery modeling as well as DC/DC converter topologies are presented in this section. Section IV concerns the system sizing. The obtained results and a comparison study of simulation results with datasheet and experimental results are given in Section V. Last section concludes the paper and gives some future directions of this work.

II. Energy Storage Sources

Energy storage system includes different storage technologies, electrochemical technology (battery), electrical

R. Mkahl is with the laboratory OPERA/FCLAB FR-CNRS3539, University of Technology Belfort-Montbéliard, Belfort, France (corresponding author, phone 0033695015520; e-mail: rania.mkahl@utbm.fr).
A. Nait-Sidi-Moh is with Laboratory of Innovative Technologies, University of Picardie Jules Verne, Saint-Quentin, France (e-mail: ahmed.nait-sidi-moh@u-picardie.fr).
M. Wack is with the laboratory OPERA/FCLAB FR-CNRS3539, University of Technology Belfort-Montbéliard, Belfort, France (e-mail: maxime.wack@utbm.fr).

technology (supercapacitor), and mechanical technology (a flywheel) as detailed in [4]. To compare the energy storage sources many parameters can be considered. Among these parameters we underline energy density, power density, cycle life performance, cost, environmental impact [5]. Fig. 2 illustrates the Ragone diagram of different energy storages.

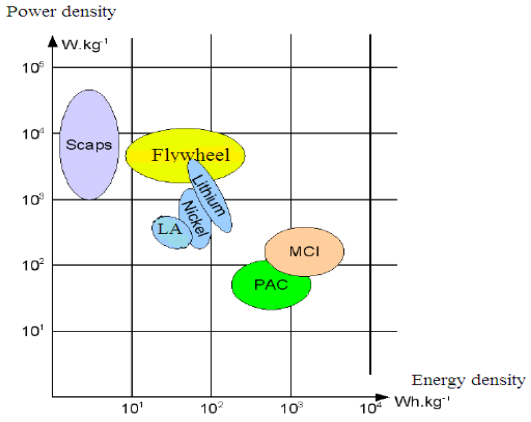

Fig. 2 Ragone plot of energy storage

This diagram shows that supercapacitors (Scaps) have a very high power density but a very low energy density. The batteries have a low power density and high energy density. The batteries are "reversible" generators; they can store electrical energy in chemical form and return it at any time when it is needed. The nature of electric vehicles is governed primarily by the characteristics of the used batteries. The weight and volume of batteries are usually a decisive factor. A BEV must satisfy certain conditions: a good specific power for high accelerations, good specific energy synonymous with good battery life, stable voltage generating regular performances, a long lifetime and low maintenance and recyclable [6].

Batteries currently used in electric vehicles are: Lead-Acid (LA) battery, Lithium-Ion (Li-Ion) battery, Nickel Metal Hybrdrure [7], Nickel Cadmium battery [6], and Zink-Air. Li-Ion battery is the main hope for electric vehicles [8]. It holds a higher voltage per element, good volume and mass performance, and a very high specific energy compared to other types of batteries. It is worth noting that the specific systems of stationary electricity storage are very different from the specific systems of embedded systems for which energies and unit powers are weak. In stationary systems, the amount of energy and the total power available then become largely predominant. Lead-Acid batteries have high availability and they are the least expensive storage batteries for any application, while still providing reasonable performance and life characteristics. They are widely used like the stationary electricity storage in PV systems as given in [9].

III. Modeling of the System Components

In this section, we focus on the modeling of the main components of charging station. To do so, we present PV and Lead-Acid battery models and DC/DC converter topologies.

A. PV Modeling

Several studies are developed about the mathematical modeling of the PV cell. A model of the photovoltaic cell with double diode is developed in [10]. This model consists of a current source representing the light flux, in parallel with two diodes. The diode represents the cell behavior in darkness. Tow resistances, shunt and series resistance are added to present internal losses. The current-voltage (I-V) equation can be simplified by considering the shunt resistance as infinity [11]. Another works have been proposed to simplify the PV cell by using single-model PV cell with one diode [12]. Like this last research work, we use a single-model PV cell in order to formalize the PV solar cell. The equivalent electrical circuit is presented in Fig. 3.

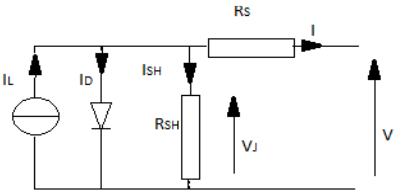

Fig. 3 Equivalent circuit of a solar cell

The equation of PV module witch expresses the characteristic current–voltage (I-V) of PV module is given as follow [13]:

$$I_m(t) = n_p \times \left(I_L(t) - I_0 \left[\exp\left(\frac{q(V(t) + I_m(t)R_{Sm}/n_p)}{n_s \times nkT} \right) - 1 \right] - \left(\frac{V(t) + I_m(t)R_{Sm}}{n_p \times R_{SHm}} \right) \right) \quad (1)$$

n: diode ideality factor (1 for an ideal diode); n_s: cells in series n_p: cells in parallel; I_m: current of PV module; V: voltage of PV module; R_{Sm}: series resistance of PV module; R_{SHm}: shunt resistance of PV module; I_L : photovoltaic current; I_0: reverse saturation current; $\frac{KT}{q}$: terminal potential (0.0259V at 25C°).

Generally, unless otherwise specified by the manufacturer, PV module consists of thirty six cells in series (n_s =36 cells) and n_p=1 cell. The PWX500-12V module is chosen for this study. The parameters I_0, R_{Sm}, R_{SHm} of this module are not given in the data sheet, so we have determined it by using the functions 'fittype' and 'fit' of Matlab. The parametric identification is considered by using current-voltage (I-V) characteristic curve of the module extracted from experimental data. The PV panel parameters are reported in the Table I.

TABLE I
PV Parameters

PV parameters	Digital values
R_{Sm}	0.2297 Ω
R_{SHm}	60.78 Ω
I_0	3.886e-009 A

B. Lead-Acid Battery Modeling

1. Voltage Modeling

In the literature the battery behavior has been described by many models. In fact, several research works proposed some

battery models which describing battery behavior for specifics purpose, from the battery design and performance estimation to the circuit simulation. According to these researches, the battery models can be classified into three categories:

The electrochemical model: this model is used to optimize the physical design aspects of batteries, to characterize the fundamental mechanisms of power generation and lay electric parameters of the battery with chemical parameters [14]. Shepherd model which can be considered as the best battery model for using for the hybrid vehicle analysis is one example of electrochemical model [15].

The mathematical model is the second category. This model is mostly too abstract to embody any practical meaning but it is useful to system designers [16]. Ciemat model is one example of a mathematical model. This model consists of an ideal voltage in series with resistance, the electromotive force and resistance which are expressed according to the battery SOC as detailed in [17].

The third category is electric model. This last lies between electrochemical and mathematical model. Electric model consists of voltage source in series with a resistance which is not function of battery SOC [18].

The goal of this section is to determine a relationship between the battery voltage and the battery time charging/discharging. This expression takes into account the electrical parameters. During cycles of charging and discharging, the characteristics of the battery depend on its SOC, charging/discharging current and charging/discharging time. As given in [19], the SOC of the battery is defined by:

$$soc = soc_0 - \frac{1}{c_n}\int i(t)dt \tag{2}$$

where: SOC_0: initial state of charging percentage; C_n: battery capacity in Ampere-hours; i(t): battery current.

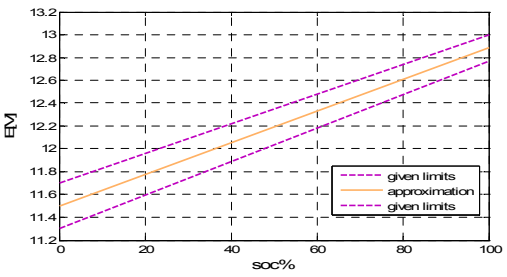

Fig. 4 Voltage E versus SOC

In the H2V concept the Lead-Acid battery YUASA SW280 was used, the nominal voltage is 12V and the capacity C_n is 7,6 Ah, for n = 20. The effect of temperature on discharging curves is not given by the datasheets, so the modeling is done at a temperature of 20°C.

As exposed in [20], datasheets give the relationship between E (open circuit voltage) and SOC (State of Charge). For the battery YUASA SW280 this relationship is linear as illustrated in Fig. 4. A mathematical equation of SOC according to E is established using a linear approximation technique as detailed in [21].

Based on the curves showing the evolution of the terminal voltage discharging, we deduce an expression of the voltage discharging battery by an extrapolation of the points which have been raised.

For charging curve, the datasheet does not give sufficient curves. So, we charge the battery with constant current in order to obtain the curve enabling to describe the relationship between the terminal battery voltages during charging versus charging time. The battery is charged with constant current I_1 until the battery voltage reaches overcharge voltage. Then it discharges at constant current until the battery voltage dropped to the deep-discharge protection point. We repeat these processes with currents I_2, I_3,..., I_n. Finally, the obtained curves, from performed tests, describe the variation of the battery terminal voltage during charging/discharging process over the time. Based on the test data we deduce an expression of the voltage charging battery by an extrapolation of the point which we have raised.

From the datasheet, we obtain the curves and with applying the method of extrapolation of the curve, we obtain a polynomial equation of 3rd degree.

$$V(t) = At^3 + Bt^2 + Ct + D \tag{3}$$

where A, B, C, and D are the parameters of the battery whose expressions are detailed in the following subsection. It is worth noting that the parameters A, B, and C depend on the battery current. The parameter D depends on the battery current and the open circuit voltage.

2. Identification of Parameters A, B, C, D

Using basic fitting technique, the parameters A, B and C are given as polynomial functions of 7th degree depending on the battery current I. These parameters can be determined by:

- Case of charging: A= a*e-07; B = b; C = c.
- Case of discharging: A = (4, 63e-13)*a;

$$B = (2,7778e\text{-}009)*b;\ C = 0,016667*c$$

where a, b and c are given by:

$$\begin{pmatrix} a \\ b \\ c \end{pmatrix} = M\,V^t \tag{4}$$

where the vector V is given by:

$$V = [I^7, I^6, I^5, I^4, I^3, I^2, I, 1]$$

The matrix M is given by Least Square Fitting as detailed in [21].

The parameter D represents the starting voltage (voltage at the beginning of charging/discharging). Experimentally, the expression of this parameter is given by:

$$D = E \pm dv \tag{5}$$

where E is the open circuit voltage, dv is the initial voltage drop at the switching on process in the battery.

We use the sign "+" (respectively "-") in the case of the battery charging (resp. discharging). The initial voltage drop at the switching on process in the battery is given by:

$$dv = RI \tag{6}$$

R corresponds to the battery resistance which is a function of the current I. Using the technique of basic fitting we can find the relationship between R and I. We measure the values of the open circuit voltage E and the values of the starting voltage V_0 of the battery, then we find dv = E-V_0. For several values of dv, using (6), we calculate the resistance values for each corresponding values of dv, and then we find the relationship between R and I using interpolation method. This calculation is detailed in [21].

C. DC/DC Charger Topologies

Solar energy is converted to electric energy by the PV panels. Electric energy is used for recharging Lead-Acid batteries via DC/DC Boost converter (see Fig. 5(a)). Boost converter is controlled by maximum power point tracking algorithm (MPPT) for obtaining always the PV maximum power at PV panel output.

In addition, a Buck- Boost (current-bidirectional converter) is used for charging embedded Li-Ion battery into the EV from home energy (H2V). This converter can be used also for charging Lead-Acid batteries from vehicle battery (V2H) when it is needed. Fig. 5 (b) corresponds to a DC-DC current-bidirectional converter.

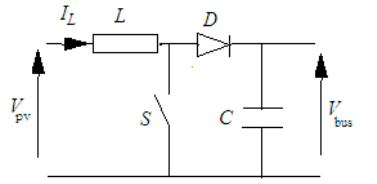

(a) boost

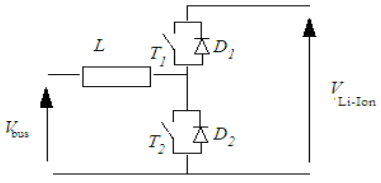

(b) Buck-Boost

Fig. 5 DC-DC charger topologies

Fig. 6 shows the fast recharge control technique consisting on a current control from low $SOC_{Li\text{-}Ion}$ to 80% and then switching to a voltage control from 80% to 100% of $SOC_{Li\text{-}Ion}$.

IV. System Sizing

In this section, we focus on the sizing of charging station for small car following a flat road.

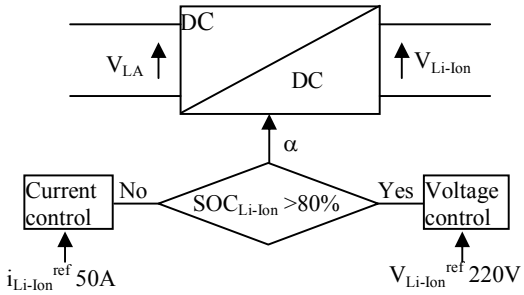

Fig. 6 Combined recharging cycle

A. Ev Sizing

The power demand is due to speed variations, tire friction dissipation, aerodynamics dissipation, and mass elevation. This power demand can be expressed as in [22] by:

$$P = V\left(C_r Mg\cos(\alpha) + Mg\sin(\alpha) + M\frac{dV}{dt} + \frac{1}{2}\rho S C_x V^2\right) \tag{7}$$

where V: vehicle speed; M=1000 (kg): vehicle mass; α = 0 (radians): road angle with a horizontal line; g = 9.81M·s^{-2}: acceleration of gravity; C_r = 0.01: friction coefficients; C_x = 0.30: aerodynamic coefficients; ρ = 1.225 (km. m^3): air density; S = 2.5(m^2): front surface area.

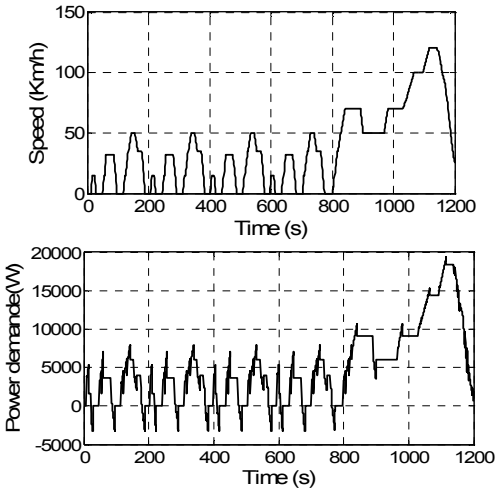

Fig. 7 NEDC driving cycle

So the vehicle energy demand equals to 17kWh. This amount of energy needs to be embedded and stored in the Li-Ion batteries pack. For testing vehicles, driving cycles have been normalized. European light-duty vehicles have to face the New European Driving Cycle (NEDC). The NEDC consists of 4 repeated urban cycles (ECE-15) and an Extra-Urban driving cycle. Fig. 7 shows the NEDC driving cycle with the speed and the power demand of the small car.

B. Sizing of PV Panels

Data of PV sizing are given in Table II. Characteristics and sizing PV panels are reported in Tables III and IV. PV panels are supposed to be installed on the roof and have a good orientation for capturing a maximum solar radiation.

TABLE II
DATA VALUES FOR PV SIZING PV PARAMETERS

Data	Values
Device	EV
Power of receiver	4704 W
Usage time	6 h
Factor Corrector	1.3
Radiation	5 k Wh/m².j

TABLE III
CHARACTERISTICS OF SOLAR PANEL PWX500-12V

PWX500-12V Characteristics	Digital values
Power max	50 W
Optimal current	2.9 A
Optimal voltage	17.2 V
Short circuit cure	3.2 A
Open circuit volt	21.6 V

TABLE IV
SIZING OF SOLAR PANEL PWX500-12V

PWX500-12V Sizing	Digital values
Number of PV panels	148
Surface of PV	70 m^2
Power max	7.4 kWc
Weight	1361 kg

C. Sizing of Lead-Acid Battery

As underlined previously we use of YUASA SW280 Lead-Acid battery as the embedded battery at home. Its characteristics are reported in Table V, and sizing results are presented in Table VI.

TABLE V
CHARACTERISTICS OF LEAD-ACID BATTERIES YUASA SW280

YUASA SW280 Characteristics	Digital values
Voltage	12 V
Volume	151x65x99 mm
Weight	2.7 kg
Nominal capacity	7.6 Ah
Energy / Volume	93 Wh/l
Energy/Weight	30 Wh/Kg
Internal resistance of charged battery	15 Ω
Maximum discharge current in minute	50A

TABLE VI
SIZING OF LEAD-ACID BATTERIES

YUASA SW280 Sizing	Digital values
N° in series	4
N° in parallel	78
Pack voltage	48 V
Pack capacity	588 Ah
Pack mass	842.4 kg

V. SIMULATION AND EXPERIMENTAL RESULTS

The simulation platform of PV system consists of PV panels, Lead-Acid batteries, Boost converter and MPPT P&Q as illustrated in Fig. 8. Hereafter, we present simulation results of PV model and we report a benchmarking with datasheets and experimental results.

A. PV Simulation Results

I-V characteristics of a PWX500-12V module are simulated according to (1). The simulation results are compared with datasheets for several levels of the radiation. Fig. 9 shows the superposition of the characteristic curves of PV panels I = f(V) with a cell temperature = 25°C and solar radiation at 5 levels: 1000W/m^2, 800W/m^2, 600W/m^2, 500W/m^2, 400W/m^2.

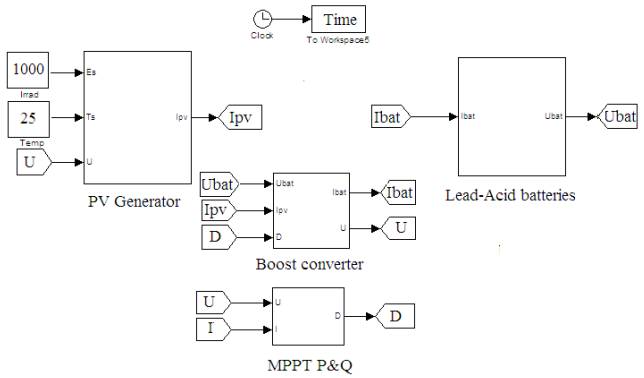

Fig. 8 PV system controlled by MPPT algorithm

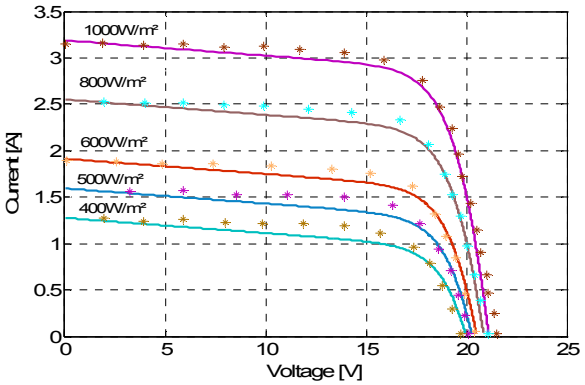

Fig. 9 Comparison of simulation results with datasheets for several levels of radiation and at cell temperature of 25°C

Fig. 9 shows that the simulation results match with those of the datasheet. After comparing the simulation results with the datasheet, we compared the simulation results with experimental results of current-voltage (I-V) characteristics and power-voltage (P-V) characteristics. The used materials for experimental tests are PWX500-12V module, variable load, current sensor, voltage sensor, contact thermometer, and light meter as illustrated in Fig. 10. The aim of these tests is to determine the I-V, P-V curves of the PV panel and find the PV panel electric parameters from the I-V curve.

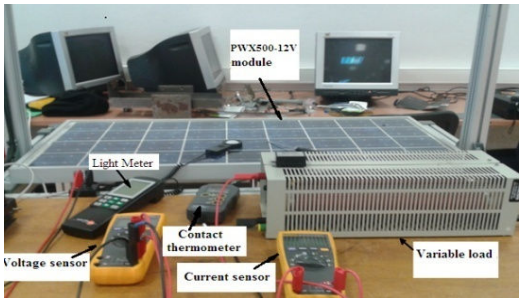

Fig. 10 Test bench of PV panel

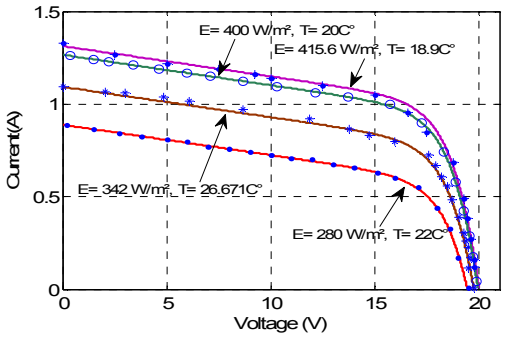

Fig. 11 Comparison I-V curves of PV model and experimental results

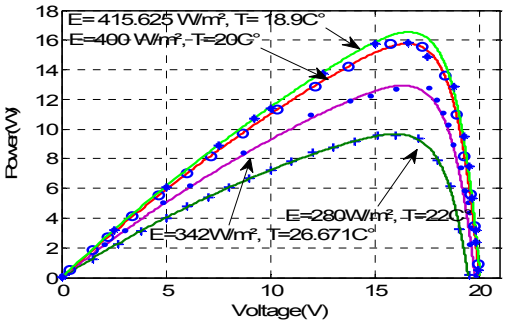

Fig. 12 Comparing P-V curves of PV model and experimental results

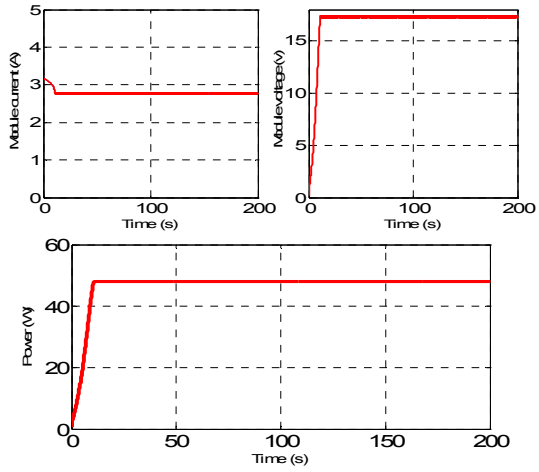

Fig. 13 PV module current, voltage and power applying MPPT algorithm

Figs. 11 and 12 show the superposition of the experimental and simulation results for the I-V and P-V characteristic curves respectively. The comparison study of the two results shows a good accuracy of this model.

The MPPT algorithm is applied to obtain the PV maximum power. Fig. 13 shows PV module current, voltage and power applying MPPT algorithm.

B. Simulation Results of Battery Lead-Acid

The work presented in this section is focused on the battery model results. Once the parameters A, B, C, and D are determined, the voltage is plotted using (3) for several current rates on the same graph compared with the curves of the datasheets, Fig. 14.

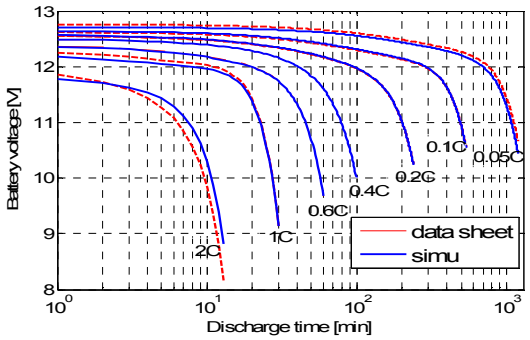

Fig. 14 Comparing the simulation of discharge voltage with the datasheet (dashed line refers to datasheet)

Based on the obtained results, absolute error and relative error are reported in Table VII. The parameter C represents the battery nominal capacity with C = 7.6 Ah.

TABLE VII
ERRORS BETWEEN DATASHEETS AND SIMULATION RESULTS

Discharging current	Absolute error	Relative error
0.05*C*	0.05	0.44%
0.1*C*	0.01	0.1%
0.2*C*	0.003	0.03%
0.4*C*	8.95.e-4	0.008%
0.6*C*	0.006	0.05%
1*C*	0.05	0.43%
2*C*	0.276	2.83%

The average error represents good model accuracy for each rate of discharging current. The simulation curves coincide with datasheets, which allows concluding that the analytical expression represents well the evolution of the terminal voltage battery YUASA SW280.

The comparison of obtained simulation results with experimental measurements for validation of the battery model accuracy is reported. Experimentations are carried out under ambient temperature. To perform the experimental tests, some materials are required such as regulated power supply for constant charge current, electronic load to discharge with constant current, acquisition card with voltage probe, PC with Labview and a current sensor. Figs. 15 and 16 show the test bench of battery test. It is worth to note that the performed tests for battery model and PV model are carried out within the laboratory FEMOT-ST/FCLAB in Belfort, a small city in the north east of France. We underline also that the PV tests are done in the first week of November 2011.

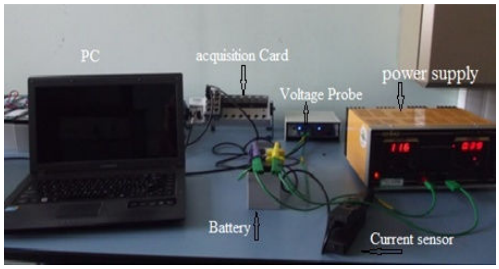

Fig. 15 Test bench of charge battery

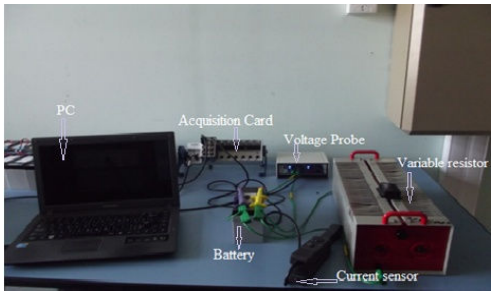

Fig. 16 Test bench of discharge battery

The proposed model enables to predict the voltage battery for discharging rate other than those given in datasheet. Fig. 17 shows results of battery discharging for I=3.22A and 2.9A.

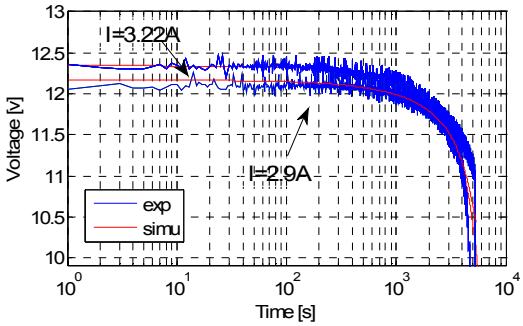

Fig. 17 Comparison of simulation and experimental results of discharging terminal voltage

In Fig. 17, we show that the experimental curves match well with those given by the analytical expression. This leads to the conclusion that the analytical expression represents well the evolution of the battery voltage Yuasa SW280.

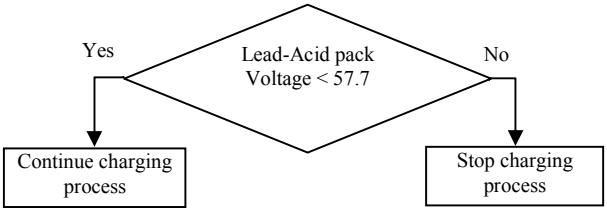

Fig. 18 Supervision system of charging Lead-Acid batteries from PV panels

Voltage and current of Lead-Acid battery with MPPT algorithm are presented in Fig. 19. W remark that the battery voltage increases until reaching the voltage of full charge and then the current switched off. The pack of batteries is fully charged for nearly 3 hours.

Fig. 20 presents the control performance in terms of current and voltage control. We can observe that the Li-Ion current is tracking its reference allowing a fast Li-Ion batteries charge (the Li-Ion battery is charged until 80% in less than 30min), than the last 20% are charged very slowly according to the Li-Ion battery characteristics (about 5 hours to obtain a full charge (100%)). Fig. 20 (b) corresponds to the Li-Ion SoC (starting from an arbitrary initial condition, 40% in this case).

The combined recharge cycle control is illustrated in Fig. 20 (a) where we can see the first value control corresponding to the current until 80% of SoC and the voltage control from 80% to 100%. Once the SoC is reaching 100%, the Li-Ion recharge is stopped and the control equals to 0 (the value of $i_{Li\text{-}Ion}$(A) in Fig. 20 (a), and the value of Alpha in Fig. 20 (c). Alpha is the temperature coefficient of the short-circuit current).

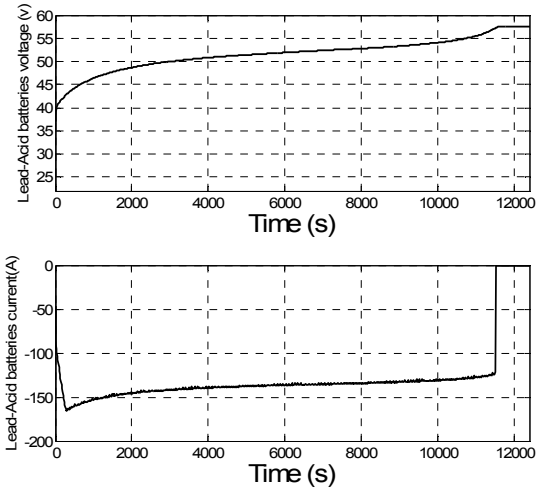

Fig. 19 Simulation of charging voltage and current pack of batteries from PV current applying MPPT algorithm

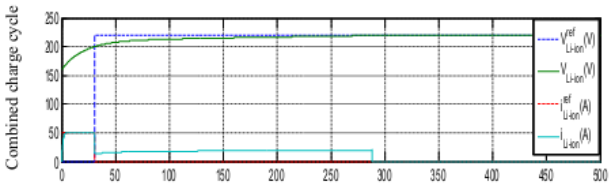

(a) Combined charge cycle vs time

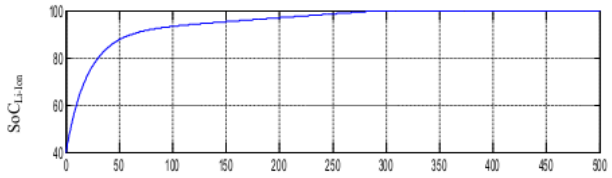

(b) SoC vs time

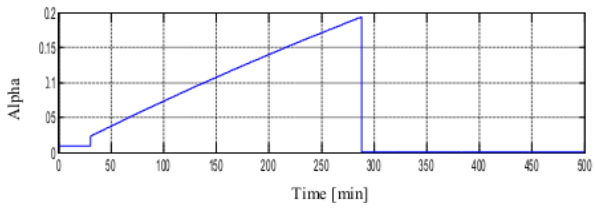

(c) Alpha vs time

Fig. 20 Li-Ion batteries charge from Lead-Acid batteries using the combined charge cycle

VI. Conclusion

To properly coordinate the operations of all elements of charging/discharging system H2V and V2H, a modeling and sizing of the whole system is required to describe and simulate the behavior of each element. In this paper, we performed a mathematical modeling of charging station for EV using solar energy; model parameters of PV panel and Lead-acid battery are identified using fitting methodology. PV and Lead-Acid models are validated experimentally. MPPT control method for obtaining PV maximum power is applied. System sizing is proposed and finally home batteries pack is charged by PV current until reaching full charging voltage. The obtained results show that the batteries Li-Ion can be charged promptly from the current of Lead-Acid batteries using buck/boost converter. In our future work, we will focus on the energy management in both directions H2V and V2H with a particular attention to bring to the battery as mean of energy storage.

References

[1] M. G. Egan, D. L. O'Sullivan, J. G. Hayes, M.J. Willers, and C.P. Henze, "Power-factor-corrected single-stage inductive charger for electric vehicle batteries," *IEEE Trans. on Industrial Electronics*, vol. 54, no. 2, pp. 1217–1226, 2007.

[2] Z. P. Wang, P. Liu, H. B. Han, C. Lu, and T. Xin, " Adistribution model of electric vehicle charging station," *Applied Mechanics and Materials*, 44–47, pp. 1543–1548, 2011.

[3] A. Ruzmetov, A. Nait Sidi Moh, M. Bakhouya, J. Gaber, and M.Wack, "Optimal assignment and charging scheduling of electric vehicles," *IEEE International Renewable and Sustainable Energy Conference (IRSEC'13)* Ouarzazate, Morocco, 10.1109/IRSEC.2013.6529691, pp. 537 –541, 2013.

[4] J. Song, Amir Toliyat, Dave Tuttle, and Alexis Kwasinski, "A Rapid Charging Station with an Ultracapacitor Energy Storage System for Plug-In Electrical Vehicles," *Electrical Machines and Systems (ICEMS), 2010, International Conference on*, pp. 2003-2007, 2010.

[5] J. Baker, "New technology and possible advances in energy storage," *Energy Policy*, vol. 36, pp. 4368–4373, 2008.

[6] A. Boucherit, " Conception d'un convertisseur de puissance pour les véhicules électriques multi-sources," Ph. D thesis of University Technologie de Belfort –Montbéliard, 2011.

[7] J. P. Trovão, P. G. Pereirinha, and H. M. Jorge, "Design Methodology of Energy Storage Systems for a Small Electric Vehicle," *World Electric Vehicle Journal,* vol. 3, pp. 1–12, 2009.

[8] A. Nouh, "Contribution au développement d'un simulateur pour les véhicules électriques routiers," Ph. D. thesis, University of Technologie Belfort-Montbeliard 2008.

[9] A. Cherif, M. Jraidi, and A. Dhouib, "A battery ageing model using in stand-alone PV systems*," Journal of Power Sources*, vol. 112, no. 1, pp. 49–53, 2002.

[10] A. Zegaouia, P. Petita, M. Ailleriea, J-P. Sawickia, and J.P Charlesa, " Experimental Validation of Photovoltaic Direct and Reverse Mode Model. Influence of Partial Shading*," Energy Procedia,* vol. 18, pp. 1247–1253, 2012.

[11] J. Surya Kumari, and Ch. Sai Babu, "Mathematical modeling and simulation of photovoltaic cell using Matlab-Simulink environment," *International Journal of Electrical and Computer Engineering*, vol. 2, no. 1, pp. 26–34, 2012.

[12] E. Mboumboue, and D. Njomo, "Mathematical modeling and digital simulation of PV solar panel using Matlab software," *Inter. Journal of Emerging Technology and Advanced Engineering,* vol. 3, pp. 24–23, 2013.

[13] S. AGBLI, "Modélisation multiphysique des flux énergétiques d'un couplage photovoltaïque-électrolyseur PEM–Pile à Combustible PEM en vue d'une application stationnaire," Ph. D. thesis, University of Franche comté 2012.

[14] N. Achaibou, M. Haddadi, and A. Malek, "Modelling of lead acid batteries in PV systems," *Siencedirecte, Energy Procedia, Clean Energy Solutions for Sustainable Environment (CESSE),* vol. 18, pp. 538–544, 2012.

[15] W. Zhoua, H. Yanga, and Z. Fang, "Battery behaviour prediction and battery working states analysis of a hybrid solar–wind power generation system," *Siencedirecte, Re-newable*, vol. 33, pp. 1413–1423, 2008.

[16] R.A Jackey, "A Simple effective lead-acid battery modelling process for electrical system component selection," SAE Technical Paper, 2007.

[17] O. Geraud, G. Robin, B. Multon, and H. Ben Ahmed, "Energy modeling of a lead-acid battery within hybrid wind/photovoltaic systems," *European Power Electronic Conference 2003*, Toulouse, 2003.

[18] M. Dürr, A. Cruden, S. Gair, and J.R. McDonald, "Dynamic model of a lead acid battery for use in a domestic fuel cell system," *Siencedirecte, Journal of Power Sources,* vol. 161, pp. 1400–1411, 2006.

[19] M. Coleman, C. K. Lee, C. Zhu, and W. G. Hurley, "State-of-charge determination from EMF voltage estimation: Using impedance, terminal voltage, and current for lead-acid and lithium-ion batteries," *IEEE Trans. on Industrial Electronics,* vol. 54, no. 5, pp. 2550–2557, 2007.

[20] Yuasa Battery, "SWL Batteries stationnaires étanches au plomb à recombinaison de gas régulées par soupapes," 2010.

[21] R. Mkahl, and A. Nait Sidi Moh, "Modeling of charging station batteries for electric vehicles*," J. of Asian Electric Vehicles*, vol. 11, no. 2, pp. 1667–1672. 2013.

[22] M. Becherif, M. Y. Ayad, D. Hissel, and R. Mkahl, "Design and sizing of a stand-alone recharging point for battery electrical vehicles using photovoltaic energy," *IEEE Vehicle Power and Propulsion Conference*, 10.1109/VPPC.2011.6043075, pp. 1–6, 2011.

[23] A. Ruzmetov, A Nait-Sidi-Moh, M. Bakhouya, and J Gaber, "A (max - plus)-based approach for charging management of electric vehicles*," In Proc. of the 2nd World Conference on Complex Systems,* Agadir, Morocco. Nov. 2014.

Rania, Mkahl is a PhD student working at the University of Technology Belfort-Montbéliard (UTBM), Belfort, France. Her PhD thesis is part of research collaboration between the UTBM and the University of Picardie Jules Verne (UPJV) – INSSET, Saint Quentin, France. She received her Master's degree in Electrical Engineering from the Ecole Centrale of Lyon, France in 2010. Prior to beginning the Master and PhD programs, she worked as assistant professor at the Tishreen University, Syria. Her main research interests are modeling, control and management of energy flows H2V and V2H, charging process of electric vehicles, renewable energy for EV charging, decision-making, simulation and operations research.

Ahmed, Nait-Sidi-Moh received his Ph.D. degree in 2003 in Computer Engineering and Automatic Control from the University of Technology of Belfort Montbéliard (UTBM), France. He is currently an Associate Professor of Computer Engineering at the University of Picardie Jules Verne (UPJV). Prior to joining the UPJV, he was research scientist and lecturer at the UTBM.

He has more than six years' experiences in participating and working in European and national/regional projects. He is principal investigator of a regional project Com-SloT (Community of logistic services on the Internet of Things, 2013-2016). He was Co-PI (UTBM side) of two European projects ASSET (Advanced Safety and Driver Support in Efficient Road Transport, FP7-SST, 2008-2011, and TELEFOT (Field Operational Tests of Aftermarket and Nomadic Devises in Vehicles, FP7-ICT, 2008-2012. He is also a member (UTBM side) of EU EACEA Erasmus Mundus project TARGET (Transfer of Appropriate Requirements for Global Education and Technology), 2011-2014.

His research interests include modeling, analysis and control of discrete event systems, resources and information sharing, decision-making and interoperability for service composition, Internet of Things, Geo-positioning and mobility, decision-making and management of EV charging.

Maxime, Wack received his PhD degree in 1981 in computer science from the Université de Technologie de Compiègne (UTC), France. Currently, he is associate professor-HDR (Habilité à diriger les recherches) at the laboratory OPERA/FCLAB at the Université de Technologie de Belfort Montbéliard (UTBM). He is the head of the research group Geopositioning, Embedded systems and mobility (GSEM) at UTBM.

He was Co-PI of two European projects ASSET (Advanced Safety and Driver Support in Efficient Road Transport, FP7-SST, 2008-2011, and TELEFOT (Field Operational Tests of Aftermarket and Nomadic Devises in Vehicles, FP7-ICT, 2008-2012. He is also a member (UTBM side) of EU

EACEA Erasmus Mundus project TARGET (Transfer of Appropriate Requirements for Global Education and Technology), 2011-2014.

His research interests include information systems, security, digital signature and certification, ubiquitous and pervasive computing, location based services and distributed systems, energy.